Carboxyl groups trigger the activity of carbon nanotube catalysts for the oxygen reduction reaction and agar conversion

Yexin Zhang[1], Chunlin Chen[1], Lixia Peng[2], Zhongsen Ma[1], Yajie Zhang[1] (✉), Hengheng Xia[1], Aili Yang[2], Lei Wang[1] (✉), Dang Sheng Su[3], and Jian Zhang[1] (✉)

[1] *Ningbo Institute of Materials Technology & Engineering, Chinese Academy of Sciences, Ningbo 315201, China*
[2] *Science and Technology on Surface Physics and Chemistry Laboratory, Mianyang 621907, China*
[3] *Institute of Metal Research, Chinese Academy of Sciences, Shenyang 110016, China*

Received: 09 September 2014
Revised: 24 November 2014
Accepted: 30 November 2014

KEYWORDS
carbon nanotubes,
functionalization,
carboxyl group,
oxygen reduction reaction,
biomass conversion

ABSTRACT

Ozone treatment is a common way to functionalize commercial multi-walled carbon nanotubes (CNTs) with various oxygen functionalities like carboxyl, phenol and lactone groups, in order to enhance their textural properties and chemical activity. In order to detail the effect of each functional group, we correlated the activity with the surface density of each group, and found that the carboxyl groups play a pivotal role in two important catalytic reactions, namely the electrochemical oxygen reduction reaction (ORR) and agar conversion to 5-hydroxymethylfurfural (HMF). During the processes, the hydrophilic surface provides a strong affinity for reaction substrates while the improved porosity allows the efficient diffusion of reactants and products. Furthermore, the activity of functionalized CNTs for agar conversion remained almost unchanged during nine cycles of reaction. This work highlights a strategy for improving the activity of CNTs for electrochemical ORR and agar conversion reactions, as well a promising application of carboxyl-rich CNTs as a solid acid catalyst to produce high-purity HMF—an important chemical intermediate.

1 Introduction

Carbon nanotubes (CNTs) have attracted tremendous interest in many important fields such as catalysis, fuel cells, lithium batteries, composite materials and electric devices [1–3]. Surface functionalization with oxygen, nitrogen and other heteroatoms has proved to be an efficient way to significantly improve the performance of CNTs due to the enhanced compatibility and surface reactivity. For instance, a variety of surface oxygen groups can play a key role in many heterogeneous and homogeneous reactions. Zhang

et al. [4] proposed that ketonic C=O groups can abstract hydrogen atoms from the C–H bands of alkanes to produce the corresponding alkenes and Aguilar et al. [5] found that alkaline ketone/benzoquinone groups as active sites were responsible for the oxidation of aqueous ammonia. In addition, the carboxyl group has been suggested to be the active site for phenol oxidation [6]. Oxygen functional groups on carbon have also been reported as participating in the electrochemical oxygen reduction reaction (ORR) [7–10]. After incorporating a number of acidic components such as sulfonic acid groups, carbon materials have been found to display a high activity for the conversion of biomass into 5-hydroxymethylfurfural (HMF)—an important chemical intermediate for the synthesis of biopolymer materials [11–13]. However, despite many studies of the effect of functional groups on CNTs in catalysis, the effect of a specific group on the catalytic turnover is still unclear. In particular, although the carboxyl group has a high acid strength there have been no reports of its use in electrochemical oxygen reduction and biomass conversion—two attractive topics in the field of sustainable chemistry.

In this work, commercial multi-walled CNTs were treated by a diluted flow of ozone to grow various oxygen functional groups. The distribution of oxygen-containing groups was quantified by X-ray photoelectron spectroscopy (XPS) and the Boehm titration method, and the activities for electrochemical ORR and agar conversion to HMF were evaluated. Furthermore, these activities were correlated with the distribution of oxygen functional groups to investigate the structure–performance relationship. We were delighted to observe the key role of the carboxyl groups in both reactions, and the results may provide a clear clue to optimize the structure of carbon catalysts and promote further fundamental research into metal-free catalysis.

2 Experimental

2.1 Materials

The pristine multi-walled CNTs (MWCNTs) prepared by a chemical vapor deposition method (purity 97.5 wt.%, average diameter 12.9 nm, length 3–12 μm) were supplied by Shandong Dazhan Nanomaterials Co., Ltd., China. The ozone was produced by an O_3 generator (WH-H-Y, WAOHUANG OZONE Mechanical and Electrical Equipment Co., China) using pure oxygen as the gas supply.

2.2 Functionalization of MWCNTs with ozone oxidation

Generally, the pristine CNTs (2 g) were placed into a quartz boat inside a tube furnace. Ozone (3.6 vol.% in an O_3/O_2 mixture) with a flow rate of 0.5 L/min was continuously passed through the reactor chamber at different temperatures (25–200 °C). The oxidation process was carried out for 2 h and the functionalized samples are denoted as CNT-*x*, in which *x* represents the treatment temperature in Celsius degree.

2.3 Characterization

The overall oxygen content of each sample was evaluated by an organic elemental analyzer (OEA) (HORIBA EMGA-620W). XPS tests were carried out on an AXIS ULTRADLD Multifunctional X-ray photoelectron spectroscope with an Al Kα radiation source at room temperature and under a vacuum of 10^{-7} Pa (10^{-9} Torr). The starting angle of the photoelectrons was set at 90°. The spectrum was calibrated with reference to the C1s peak at 248.6 eV. N_2 adsorption/desorption isotherms at 77 K were measured with a Micromeritics ASAP 2020 instrument after outgassing samples at 80 °C for 30 min prior to analysis. The specific surface areas were calculated with the Brunauer–Emmett–Teller (BET) equation. The pore size distributions (PSD) were obtained by the Barrett-Joyner-Halenda (BJH) method using the desorption branch of the isotherms.

2.4 Boehm titration

The amount of oxygen functional groups was quantified by the Boehm titration method [14, 15]. The number of various groups was calculated under the following assumptions: NaOH can neutralize lactone, carboxyl and phenol groups; Na_2CO_3 can neutralize both lactone and carboxyl groups; $NaHCO_3$ can only neutralize carboxyl groups. The difference between the uptakes of the bases can be used to quantify each

specific oxygen group. A mass of ca. 0.5 g sample was added to one of three bases (25.0 mL, 0.03 M): $NaHCO_3$, Na_2CO_3 and NaOH, which were analytical grade reagents (> 99.0%, Sinopharm Chemical Reagent Co., Ltd). The solution was agitated for 24 h and then filtered to remove the samples. The filtrate was titrated by hydrochloric acid (Sinopharm, 0.03 M) with degassing by pure N_2 to ensure complete CO_2 expulsion. During the titration, the pH change was recorded and the endpoint was determined from the first derivative of the pH–volume plot.

2.5 Cyclic voltammetry (CV)

All electrochemical tests were carried out with a CHI 760E electrochemistry workstation (Shanghai CH Instruments, China) and a conventional three-electrode test cell at 25 ℃. The counter and reference electrodes were a graphitic rod and a 3 M Ag/AgCl, respectively. The glassy carbon disk was polished with 30 nm alumina powder, sonicated and rinsed with deionized water and ethanol before use. The homogeneous catalyst ink was prepared by ultrasonically dispersing a mixture of 1 mg of catalyst, 50 μL of a 5 wt.% Nafion solution in alcohol, and 400 μL of H_2O. 5 μL of catalyst ink was subsequently pipetted and spread on a 3 mm-diameter pre-cleaned glassy carbon disk as the working electrode. All electrolyte solutions were deaerated by ultrapure N_2 for at least 15 min prior to any measurement. To evaluate the catalytic activity for ORR, the cyclic voltammetry experiments were carried out in 0.1 M KOH solution saturated with ultrapure O_2 (20 mL·min^{-1}) at a scan rate of 100 mV·s^{-1}.

2.6 Rotating disc electrode (RDE) experiments

A working electrode was fabricated by pasting a 20 μL aliquot of the catalyst ink prepared as above on a glassy carbon rotating disk electrode (5 mm in diameter, from PINE Instruments, USA), yielding an approximate catalyst loading of 40 μg. The electrolyte was 0.1 mol·L^{-1} KOH solution, the counter and the reference electrodes were an artificial graphite electrode and Ag/AgCl electrode, respectively. Linear scanning voltammetry (LSV) tests were performed at rotation speeds of 1,600 rpm in an O_2-saturated electrolyte at a sweep rate of 10 mV·s^{-1}.

2.7 Conversion of agar to HMF

In a typical run, agar (0.125 g) was dissolved in 2 mL of deionized water, giving a solution of agar with a concentration of 79 g·L^{-1}. Then, catalyst (0.1 g) was added and reaction mixture was heated to 120 ℃ in a closed reactor with an oil bath, and the conditions were maintained for a given reaction time. After the desired reaction time elapsed, the water loss was complemented. The solution was separated by centrifugation at 5,000 rpm and then analyzed by high performance liquid chromatography (HPLC, Agilent ZORBAX). In the recyclability tests, the separated catalyst was washed by deionized water for the next cycle. Also, the performance of acetic acid (AC) for agar conversion was compared. 2 mL of AC with different concentrations of 100%, 50% and 0.25% was mixed with 0.125 g of agar, with the subsequent operations carried out as above.

3 Results and discussion

3.1 Oxygen analysis

We first prepared a variety of CNT samples with different amounts of each functional group. The solution-free ozone treatment is a clean and effective way to introduce various oxygen-containing functional groups onto the carbon materials, which mainly produces CO_2 and H_2O [16]. We employed the diluted ozone to oxidize CNTs at different temperatures (25–200 ℃). The oxygen contents of the samples were determined by OEA and XPS analysis. As shown in Fig. 1(a), the trends in various oxygen group contents measured by the two techniques are almost consistent with each other. Note that the oxygen contents measured by XPS are somewhat higher than those measured by OEA, which may reflect the fact that XPS is a surface analysis technique. The pristine CNTs possessed quite low oxygen content of 1.24 and 0.24 wt.% as measured by XPS and OEA, respectively. After treatment at 25 ℃ (CNT-25), the oxygen contents sharply increased to 7.8 and 4.8 wt.%, respectively. When the temperature was elevated to 40 ℃ (CNT-40), a maximum in oxygen content (8.3 wt.% measured by XPS) was obtained. However, the oxygen content

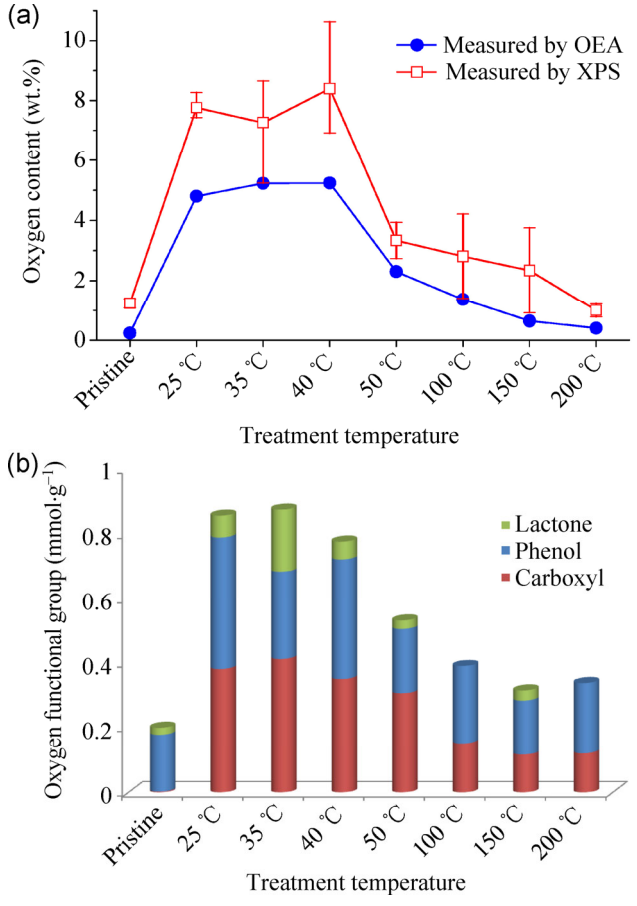

Figure 1 (a) Oxygen contents of all CNTs determined by XPS and OEA; (b) Concentrations of oxygen functional groups of all samples determined by Boehm titration.

suddenly dropped to 2.3 wt.% (OEA) at a higher temperature of 50 ℃ (CNT-50), and finally decreased to 0.41 wt.% (OEA) at 200 ℃ (CNT-200). A reasonable explanation for this is that the increased rate of decomposition of ozone to oxygen at higher temperatures reduced the efficiency of oxidation. This was verified by blank experiments without a CNT sample, which showed that the ozone decomposition became significant above 50 ℃ (see Fig. S1 in the Electronic Supplementary Material (ESM)).

In the XPS surveys of all samples (Fig. S2 in the ESM), no Fe signal was observed while C1s and O1s were present. The oxygen functional groups on carbon materials are generally distinguished and quantified by deconvolution of the high-resolution C1s or O1s XPS spectra, which may introduce arbitrary errors and lead to incorrect estimates of the populations of different oxygen functional groups [17]. In this work, we used the Boehm titration method to provide a more convincing and quantitative measure of the relative amounts of the different oxygen functional groups as shown in Fig. 1(b). To evaluate the possible disturbance of the residual metal catalyst particles contained in the CNTs framework, we used the ICP-AAS method to analyze the amount of metal ions in the titration solution. The amount of Fe ions was below 1.5×10^{-4} mmol·g_{CNTs}^{-1}, giving a negligible error of less than 4.5×10^{-4} mmol·g_{CNTs}^{-1} during the calculation of total amount of oxygen functional groups.

The trend in the total concentration of the different oxygen functional groups approximately coincided with that of total oxygen content, as shown in Fig. 1(a). The concentration of phenol groups changed irregularly with increasing temperature. In contrast, the concentration of carboxyl groups sharply increased from 0.002 to 0.414 mmol·g^{-1} as the temperature was raised to 35 ℃. Further increases in temperature suppressed the formation of carboxyl groups. An analogous phenomenon was observed by Álvarez et al. [18] in the ozone treatment of activated carbon, in which the amount of carboxyl groups produced was a maximum at 25 ℃ rather than at 100 ℃. Razumovskii et al. [19] observed by electron spin resonance (ESR) that the reaction of ozone and a graphitic matrix generates peroxide radicals. The further reaction of peroxide radicals with carbon–hydrogen bonds in the graphitic matrix may generate hydrotrioxide intermediates, which transform into the carboxyl functional groups as proposed by Chiang et al. [20]. In this work, the carboxyl groups as fraction of the overall oxygen functional groups can reach as high as 57.8% at a treatment temperature of 50 ℃, suggesting that the selective enrichment of carboxyl groups might be realized by optimizing the parameters of ozone treatment in the future.

3.2 Textural characterization

The textural structure of CNTs, characterized by N_2 isothermal physical adsorption/desorption, was significantly affected by functionalization. For the CNTs treated by ozone below 50 ℃, the BET surface area significantly increased (Fig. S3(a) in the ESM), and the optimal value of 329.7 $m^2 \cdot g^{-1}$ was obtained for CNT-40 as compared with the lower value for

pristine CNTs (219.1 $m^2 \cdot g^{-1}$). The trend in BET surface area is roughly coincident with that for the total concentration of oxygen functional groups, as shown in Fig. 1(b).

The effect of oxygen functional groups on the textural structure of CNTs is provided in detail by the profiles of pore size distribution (PSD) determined from N_2 isothermal desorption (Fig. S3(b) in the ESM). For all samples, including pristine and functionalized CNTs, there is a broad distribution between 5 and 160 nm with the most probable pore size centered at around 30 nm, which can be assigned to the splits between the bundles of CNTs. In the enlarged PSD profiles below 5 nm, as shown in Fig. 2(a), there is a PSD peak at 3 nm for all samples. These pores may be the apertures between the walls of the CNTs that are formed when they twist together [21] and are preserved on the CNTs treated by ozone. In addition, there is also a shoulder around 3.3 nm, which became intense on the CNTs treated in the low temperature region of 25–50 °C, being related to the enhanced volume of pores below 5 nm (Fig. S3(a) in the ESM). The variation

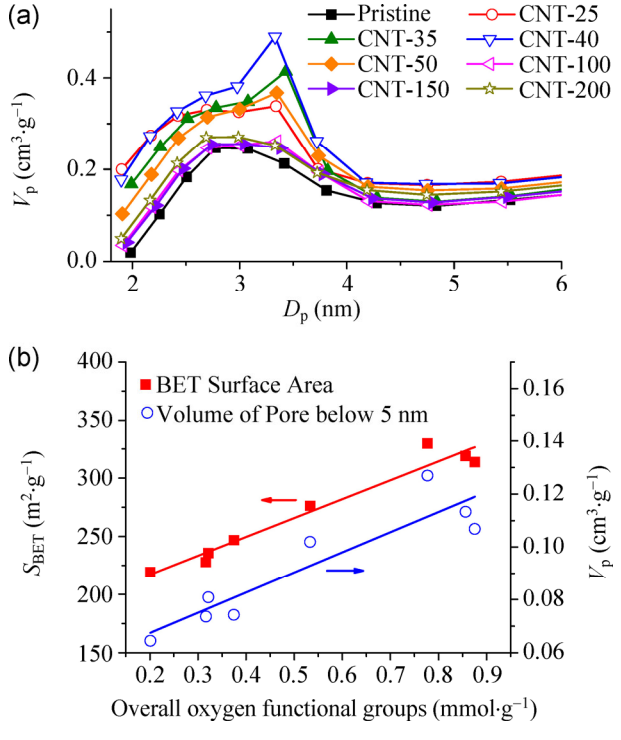

Figure 2 (a) Profiles of pore size distribution below 6 nm determined by N_2 isothermal desorption; (b) linear relationships of the BET surface area and the volume of pores below 5 nm with the total concentration of oxygen functional groups.

in pore volume also roughly coincides with that of the total concentration of oxygen functional groups. It can therefore be deduced that the enhanced pore volume after functionalization may be derived from the repulsions of oxygen functional groups, which could enlarge the apertures between the walls of CNTs twisted together, and thus increase the BET surface area.

In Fig. 2(b), both BET surface area and the volume of pores below 5 nm showed a roughly linear relationship with the overall amount of surface oxygen functional groups. The deviation of some points from the general trend may be due to the different weighting factors of the various functional groups. Therefore, two ternary linear regression models of the BET surface area (S) and volume of pores below 5 nm (V) with the concentrations of carboxyl ($C_{carboxyl}$), phenol (C_{phenol}) and lactone ($C_{lactone}$) groups were obtained as follows:

$$S = 180.04C_{carboxyl} + 195.28C_{phenol} + 59.82C_{lactone} + 176.58 \quad (1)$$

$$V = 0.12C_{carboxyl} + 0.07C_{phenol} - 0.04C_{lactone} + 0.05 \quad (2)$$

In both Eqs. (1) and (2), the larger coefficients for $C_{carboxyl}$ and C_{phenol} indicate the considerable contributions of carboxyl and phenol groups to the increased BET surface area and pore volume. This phenomenon can be understood since, unlike the lactone groups, both carboxyl and phenol groups are dangling on the surface of the CNTs.

3.3 ORR activity

The electrocatalytic capabilities of pristine and treated CNTs were evaluated for ORR by CV in 0.1 M KOH solution saturated with N_2 and O_2. In Figs. 3(a) and 3(b), CNT-40 is taken as an example for comparison with the pristine CNTs. Under N_2 protection (Fig. 3(a)), the voltammetric currents of pristine CNTs showed a featureless curve, suggesting the absence of metal impurities on the surface [22]. The CV results for CNT-40 showed a significant increase in the area, indicating that the functionalization greatly improved the capacitance of CNTs. In the presence of O_2 (Fig. 3(b)), ORR activities were observed for both samples. The pristine CNTs exhibited a well-defined peak at a potential of −0.35 V, while CNT-40 gave a peak at more

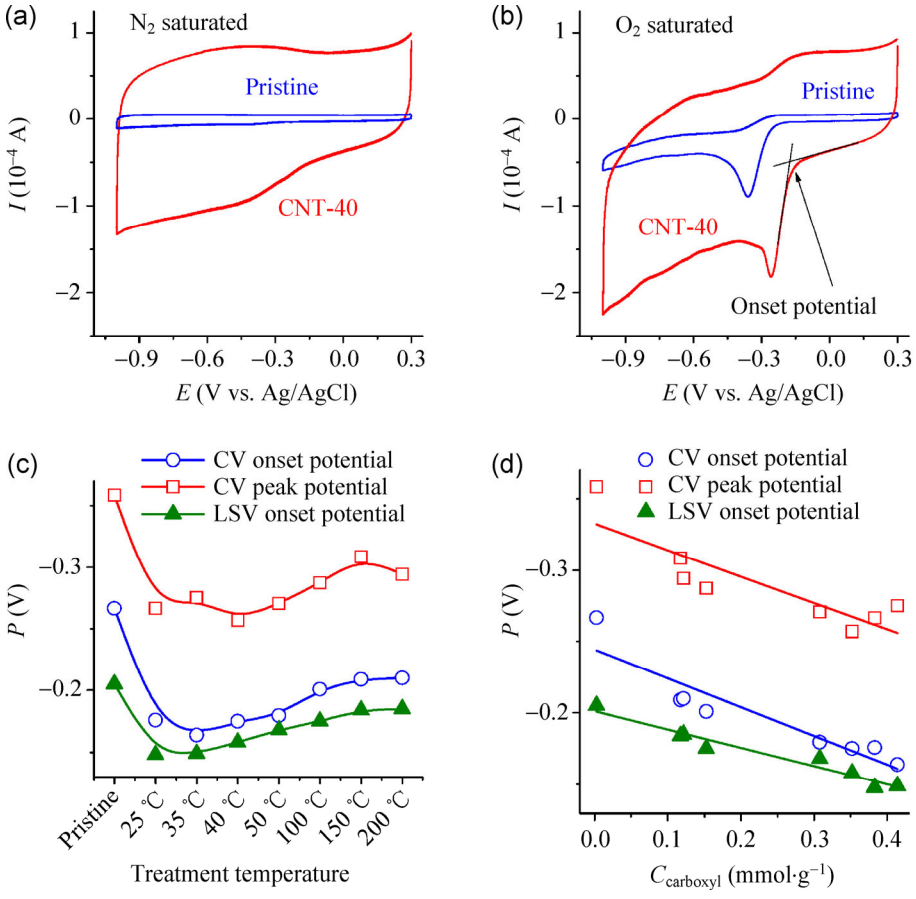

Figure 3 CVs of pristine CNTs and CNT-40 saturated with N_2 (a) and O_2 (b); (c) CV potentials and LSV onset potentials for all the CNTs; (d) linear relationships of CV potentials and LSV onset potentials with the concentration of carboxyl groups on CNTs.

positive potential (lower overpotential) of –0.26 V, suggesting an improved ORR activity.

The CV potentials, including onset potential and peak potential, of all CNTs are displayed in Fig. 3(c). The onset potential was determined by the intersection of the two tangents of the background and declining reduction currents [23] as shown in Fig. 3(b). All treated CNTs, especially the CNTs treated between 25 and 50 °C, exhibited more positive CV potentials than the pristine CNTs. The most positive onset CV potential of −0.16 V was observed for CNT-35, and the value is close to that for the sulfonic acid functionalized graphene nanoplatelets reported by Jeon et al. [24]. The ORR performances were also comparable to those of N-doped porous carbon materials [25] and some noble metals reported in the literature [26–29], indicating surface functionalization has great potential as a means to improve ORR activity (see Table S1 in the ESM).

To eliminate the diffusion limitations in ORR, RDE experiments for LSV measurements were performed. The onset potential of an LSV curve (Fig. S4 in the ESM) is defined as the potential at which the ORR current is 5% of that measured at −0.3 V [30], and the values are also displayed in Fig. 3(c). The trend in LSV onset potential approximately coincided with that for the CV potentials.

Figure 3(d) shows the linear relationships between the ORR potentials—including CV onset potential (P_{CV_onset}), CV peak potential (P_{CV_peak}) and LSV onset potential (P_{LSV_onset})—and the concentration of carboxyl groups, with the overpotentials decreasing with increasing concentration of carboxyl groups. This can be further verified by the ternary linear regression models of the ORR potentials as a function of the concentrations of the three oxygen functional groups as follows:

$$P_{CV\_onset} = 0.29C_{carboxyl} - 0.10C_{phenol} - 0.15C_{lactone} - 0.23 \quad (3)$$

$$P_{CV\_peak} = 0.29C_{carboxyl} - 0.04C_{phenol} - 0.29C_{lactone} - 0.33 \quad (4)$$

$$P_{LSV\_peak} = 0.12C_{carboxyl} + 0.03C_{phenol} - 0.01C_{lactone} - 0.21 \quad (5)$$

In Eqs. (3)–(5), the larger coefficients of $C_{carboxyl}$ suggest that the contribution of the carboxyl groups to the improved ORR activity is larger than those of the other groups.

In the recent work of Jeon et al. [24], hydrogen-, carboxylic acid-, sulfonic acid-, and carboxylic acid/sulfonic acid-functionalized graphene nanoplatelets were employed as electrocatalysts for ORR in an alkaline electrolyte. They found that the polar nature of the functional groups plays an important role in regulating the ORR efficiency, and proposed that the high polarity results in a strong affinity of the functional groups with the electrolyte and oxygen, thus inducing strong charge repulsions between the graphitic layers which allows efficient diffusion of oxygen. In this work, the dominant role of the carboxyl groups of CNTs in the improved ORR activity strongly supports their hypothesis. On the one hand, the high polarity of the carboxyl groups will enhance the surface hydrophilicity of CNTs. On the other hand, the presence of carboxyl groups and phenol groups may enlarge the apertures between the walls of CNTs twisted together. Both effects are beneficial to the electrochemical ORR activity of the CNTs.

3.4 Agar conversion to HMF

The pristine and treated CNTs were employed as the solid-acid catalysts for agar conversion to HMF. The catalytic activities of all the CNTs in agar conversion are shown in Fig. 4(a), in which the yield and selectivity of HMF were determined after reaction for 6 h. A higher HMF yield was observed over the treated CNTs than that over the pristine CNTs. The CNTs treated between 25 and 50 ℃ exhibited higher activity than others. Furthermore, the HMF yield is correlated to the amount of carboxyl groups and a linear relationship between them is observed, as shown in Fig. 4(b). Undoubtedly, the carboxyl group is active for biomass conversion to HMF, which can be justified by the fact that carboxyl group possesses the strongest acid strength among the oxygen functional groups. A linear relationship between the acid density of sulfonic groups with the activity for fructose conversion was also found by Liu et al. [12].

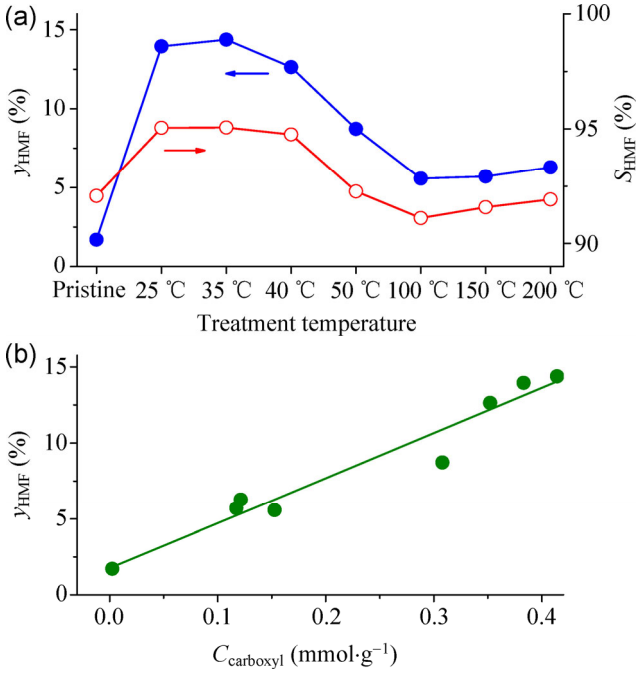

Figure 4 (a) Yield and selectivity of HMF over all CNTs for agar conversion; (b) Liner relationship between the HMF yield and concentration of carboxyl groups on CNTs for agar conversions.

In order to get an insight into the catalytic role of the carboxyl groups, the activity of CNT-25 for agar conversion was compared with that of AC with different concentrations of 100%, 50% and 0.25% in the reaction solution. Based on HMF yield, the activities decreased in the order: 50% AC > 0.25% AC > CNT-25 > pure AC (Fig. S5 in the ESM). The lowest activity of pure AC (HMF yield < 5%) may be due to the low acidity associated with the limited hydrolysis in the absence of water. Compared with 50% AC and 0.25% AC, the lower reactivity of CNT-25 may be attributed to an insufficient amount of carboxyl groups.

For clarification, the productivity of HMF was normalized to the concentration of carboxyl groups. As shown in Fig. 5(a), the obtained specific productivity for 50% AC and pure AC were close to zero, implying that most of the carboxyl groups were not utilized. The specific productivity (Fig. 5(a)) and selectivity (Fig. 5(b)) over CNT-25 were comparable to, or even slightly higher than, the corresponding values for 0.25% AC. This suggests the carboxyl groups on CNTs were fully utilized due to their high dispersion on the CNTs so that the material behaves like a homogeneous catalyst. As in the case of ORR, this can be attributed

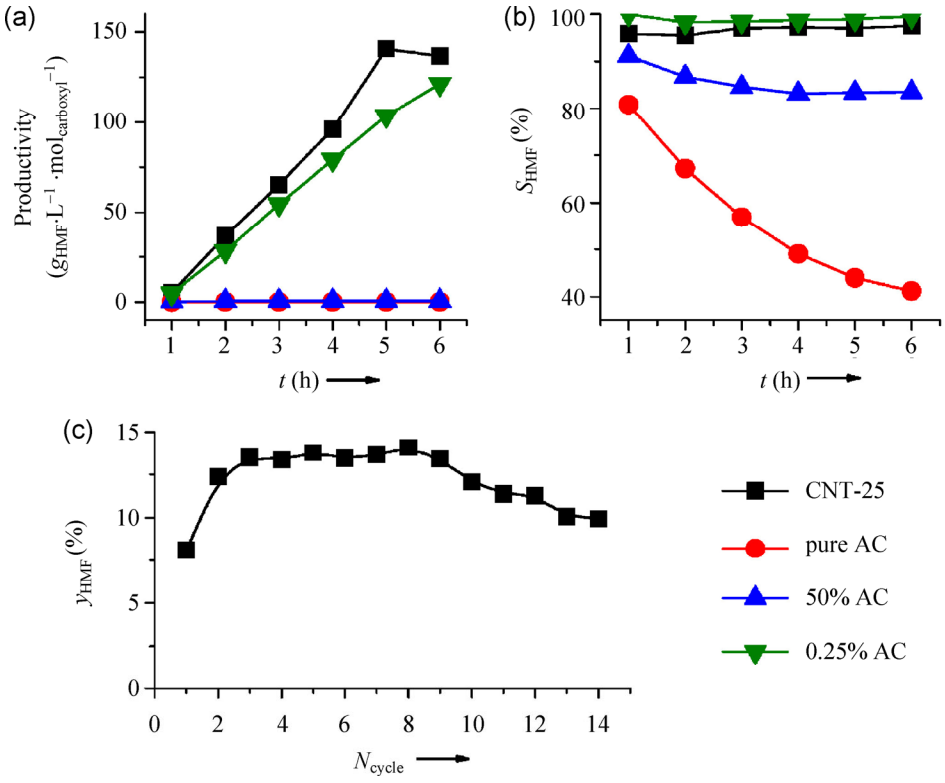

Figure 5 (a) Specific production of HMF normalized to the concentration of carboxyl groups as a function of reaction time for pure, 50% and 0.25% ACs as well as CNT-25 in agar conversion; (b) Selectivity of HMF versus reaction time in agar conversion over the above samples (c) Recyclability of CNT-25 in agar conversion for 4 h.

to the enhanced hydrophilicity and improved porosity afforded by functionalization. The former not only facilitates the dispersion of CNTs in the reaction system (aqueous solution) but also favors the affinity to the reaction substrates (agar), while the improved porosity enhances the diffusion of reaction substrates to the active sites, i.e., the carboxyl groups.

In addition, however, anchoring the carboxyl groups on CNTs offers the advantage of recyclability for heterogeneous catalytic reactions. Figure 5(c) indicates the catalytic efficiency of CNT-25 in repeated reaction cycles for agar conversion to HMF. Note that the HMF yield increased to 12.4% from 8.1% after the first reaction cycle. The lower HMF yield in the first cycle might be attributed to the HMF produced being partly adsorbed on fresh CNTs. The HMF yield in the second reaction cycle was maintained in subsequent cycles until the tenth cycle. From the tenth cycle onwards, the HMF yield decreased slowly, which may due to the loss of CNT-25 in the separation and washing processes.

4 Conclusions

Oxygen-functionalized CNTs possess high activities for ORR and agar conversion to HMF. By correlation with the distribution of oxygen functional groups, it was found that the carboxyl groups play a pivotal role in the two catalytic processes. During the reaction, the enhanced hydrophilicity affords a strong affinity with the reaction substrates while the improved porosity allows efficient diffusion of reaction substrates. Furthermore, the functionalized CNTs displayed an outstanding recyclability in agar conversion, and the performance remained almost unchanged during nine cycles of reaction. In this work, the demonstration of the dominant effect of the carboxyl groups in ORR and agar conversion will guide our future efforts to develop carboxyl-rich CNTs as solid acid catalysts, especially for the production of high-purity HMF. However, the loss of CNTs powder during the post-treatment process also emphasizes the importance of producing monolithic CNTs with good mechanical

stability before the industrialization of this catalytic process is possible.

Acknowledgements

This work was financially supported by the National Natural Science Foundation of China (Nos. 51422212, 51202262 and 21307142), the China Postdoctoral Science Foundation (Nos. 2013M531490 and 2014T70580) and the Research Fund from the Laboratory of Science and Technology on Surface Physics and Chemistry (No. ZDXKFZ201304).

Electronic Supplementary Material: Supplementary material (summary of CV experiments in some literature as well as this work, variation in outlet ozone concentration during the heating in the blank experiment, XPS surveys, BET surface areas and PSD, LSV curves, and HMF yield for agar conversion over ACs as well as CNT-25) is available in the online version of this article at http://dx.doi.org/10.1007/s12274-014-0660-3.

References

[1] Iijima, S. Helical microtubules of graphitic carbon. *Nature* **1991**, *354*, 56–58.

[2] Oberlin, A.; Endo, M.; Koyama, T. Filamentous growth of carbon through benzene decomposition. *J. Cryst. Growth* **1976**, *32*, 335–349.

[3] Baughman, R. H.; Zakhidov, A. A.; de Heer, W. A. Carbon nanotubes—the route toward applications. *Science* **2002**, *297*, 787–792.

[4] Zhang, J.; Liu, X.; Blume, R.; Zhang, A. H.; Schlögl, R.; Su, D. S. Surface-modified carbon nanotubes catalyze oxidative dehydrogenation of n-Butane. *Science* **2008**, *322*, 73–77.

[5] Aguilar, C.; García, R.; Soto-Garrido, G.; Arriagada, R. Catalytic wet air oxidation of aqueous ammonia with activated carbon. *Appl. Catal. B* **2003**, *46*, 229–237.

[6] Yang, S. X.; Li, X.; Zhu, W. P.; Wang, J. B.; Descorme, C. Catalytic activity, stability and structure of multi-walled carbon nanotubes in the wet air oxidation of phenol. *Carbon* **2008**, *46*, 445–452.

[7] Yeager, E. Dioxygen electrocatalysis: mechanisms in relation to catalyst structure. *J. Mol. Catal.* **1986**, *38*, 5–25.

[8] Hossain, M. S.; Tryk, D.; Yeager, E. The electrochemistry of graphite and modified graphite surfaces: the reduction of O_2. *Electrochim. Acta* **1989**, *34*, 1733–1737.

[9] Sarapuu, A.; Vaik, K.; Schiffrin, D. J.; Tammeveski, K. Electrochemical reduction of oxygen on anthraquinone-modified glassy carbon electrodes in alkaline solution. *J. Electroanal. Chem.* **2003**, *541*, 23–29.

[10] Vaik, K.; Sarapuu, A.; Tammeveski, K.; Mirkhalaf, F.; Schiffrin, D. J. Oxygen reduction on phenanthrenequinone-modified glassy carbon electrodes in 0.1 M KOH. *J. Electroanal. Chem.* **2004**, *564*, 159–166.

[11] Wang, L.; Zhang, J.; Zhu, L. F.; Meng, X. J.; Xiao, F. S. Efficient conversion of fructose to 5-hydroxymethylfurfural over sulfated porous carbon catalyst. *J. Energy Chem.* **2013**, *22*, 241–244.

[12] Liu, R. L.; Chen, J. Z.; Huang, X.; Chen, L. M.; Ma, L. L.; Li, X. J. Conversion of fructose into 5-hydroxymethylfurfural and alkyl levulinates catalyzed by sulfonic acid-functionalized carbon materials. *Green Chem.* **2013**, *15*, 2895–2903.

[13] Qi, X. H.; Guo, H. X.; Li, L. Y.; Smith, R. L. Acid-catalyzed dehydration of fructose into 5-hydroxymethylfurfural by cellulose-derived amorphous carbon. *ChemSusChem* **2012**, *5*, 2215–2220.

[14] Goertzen, S. L.; Thériault, K. D.; Oickle, A. M.; Tarasuk, A. C.; Andreas, H. A. Standardization of the Boehm titration. part I. CO_2 expulsion and endpoint determination. *Carbon* **2010**, *48*, 1252–1261.

[15] Oickle, A. M.; Goertzen, S. L.; Hopper, K. R.; Abdalla, Y. O.; Andreas, H. A. Standardization of the Boehm titration: Part II. method of agitation, effect of filtering and dilute titrant. *Carbon* **2010**, *48*, 3313–3322.

[16] Najafi, E.; Kim, J. Y.; Han, S. H.; Shin, K. UV-ozone treatment of multi-walled carbon nanotubes for enhanced organic solvent dispersion. *Colloids Surf. A* **2006**, *284*, 373–378.

[17] Wang, D. W.; Su, D. S. Heterogeneous nanocarbon materials for oxygen reduction reaction. *Energy Environ. Sci.* **2014**, *7*, 576–591.

[18] Álvarez, P. M.; García-Araya, J. F.; Beltrán, F. J.; Masa, F. J.; Medina, F. Ozonation of activated carbons: Effect on the adsorption of selected phenolic compounds from aqueous solutions. *J. Colloid Interface Sci.* **2005**, *283*, 503–512.

[19] Razumovskii, S. D.; Gorshenev, V. N.; Kovarskii, A. L.; Kuznetsov, A. M.; Shchegolikhin, A. N. Carbon nanostructure reactivity: Reactions of graphite powders with ozone. *Fullerenes, Nanotubes, Carbon Nanostruct.* **2007**, *15*, 53–63.

[20] Chiang, H. L.; Huang, C. P.; Chiang, P. C. The surface characteristics of activated carbon as affected by ozone and alkaline treatment. *Chemosphere* **2002**, *47*, 257–265.

[21] Li, F. X.; Wang, Y.; Wang, D. Z.; Wei, F. Characterization of single-wall carbon nanotubes by N_2 adsorption. *Carbon*

2004, *42*, 2375–2383.

[22] Gong, K. P.; Du, F.; Xia, Z. H.; Durstock, M.; Dai, L. M. Nitrogen-doped carbon nanotube arrays with high electrocatalytic activity for oxygen reduction. *Science* **2009**, *323*, 760–764.

[23] Liu, J.; Li, S. G.; Liao, W. B.; Chen, Y. A new europium(III) complex containing a neutral ligand of 2-(pyridin-2-yl)-1H-benzo[d]imidazole: Thermal, electrochemical, luminescent properties. *Spectrochim. Acta, Part A* **2013**, *107*, 102–107.

[24] Jeon, I.Y.; Choi, H. J.; Jung, S. M.; Seo, J. M.; Kim, M. J.; Dai, L. M.; Baek, J. B. Large-scale production of edge-selectively functionalized graphene nanoplatelets via ball milling and their use as metal-free electrocatalysts for oxygen reduction reaction. *J. Am. Chem. Soc.* **2012**, *135*, 1386–1393.

[25] Liu, Z. Y.; Zhang, G. X.; Lu, Z. Y.; Jin, X.Y.; Chang, Z.; Sun, X. M. One-step scalable preparation of N-doped nanoporous carbon as a high-performance electrocatalyst for the oxygen reduction reaction. *Nano Res.* **2013**, *6*, 293–301.

[26] Fu, G. T.; Liu, Z. Y.; Chen, Y.; Lin, J.; Tang, Y. W.; Lu, T. H. Synthesis and electrocatalytic activity of Au@Pd core-shell nanothorns for the oxygen reduction reaction. *Nano Res.* **2014**, *7*, 1205–1214.

[27] Neumann, C. M.; Laborda, E.; Tschulik, K.; Ward, K.; Compton, R. Performance of silver nanoparticles in the catalysis of the oxygen reduction reaction in neutral media: Efficiency limitation due to hydrogen peroxide escape. *Nano Res.* **2013**, *6*, 511–524.

[28] Si, W. F.; Li, J.; Li, H. Q.; Li, S. S.; Yin, J.; Xu, H.; Guo, X. W.; Zhang, T.; Song, Y. J. Light-controlled synthesis of uniform platinum nanodendrites with markedly enhanced electrocatalytic activity. *Nano Res.* **2013**, *6*, 720–725.

[29] Zheng, F. L.; Wong, W. T.; Yung, K. F. Facile design of Au@Pt core-shell nanostructures: Formation of Pt submonolayers with tunable coverage and their applications in electrocatalysis. *Nano Res.* **2014**, *7*, 410–417.

[30] Birry, L.; Zagal, J. H.; Dodelet, J. P. Does CO poison Fe-based catalysts for ORR? *Electrochem. Commun.* **2010**, *12*, 628–631.